Neuron
Article

Foxp-Mediated Suppression of N-Cadherin Regulates Neuroepithelial Character and Progenitor Maintenance in the CNS

David L. Rousso,[1,2,6] Caroline Alayne Pearson,[1,2] Zachary B. Gaber,[1,2,3] Amaya Miquelajauregui,[1,4] Shanru Li,[5] Carlos Portera-Cailliau,[1,4] Edward E. Morrisey,[5] and Bennett G. Novitch[1,2,3,*]
[1]Department of Neurobiology
[2]Broad Center for Regenerative Medicine and Stem Cell Research
[3]Molecular Biology Interdepartmental Ph.D. Program
David Geffen School of Medicine at UCLA, 610 Charles Young Drive East, Los Angeles, CA 90095, USA
[4]Department of Neurology, David Geffen School of Medicine at UCLA, 710 Westwood Plaza, Los Angeles, CA 90095, USA
[5]Departments of Medicine and Cell and Developmental Biology, Institute for Regenerative Medicine, University of Pennsylvania, 421 Curie Boulevard, Philadelphia, PA 19104, USA
[6]Present address: Department of Molecular and Cellular Biology, Harvard University, Cambridge, MA 02138, USA
*Correspondence: bnovitch@ucla.edu
DOI 10.1016/j.neuron.2012.02.024

SUMMARY

Neuroepithelial attachments at adherens junctions are essential for the self-renewal of neural stem and progenitor cells and the polarized organization of the developing central nervous system. The balance between stem cell maintenance and differentiation depends on the precise assembly and disassembly of these adhesive contacts, but the gene regulatory mechanisms orchestrating this process are not known. Here, we demonstrate that two Forkhead transcription factors, Foxp2 and Foxp4, are progressively expressed upon neural differentiation in the spinal cord. Elevated expression of either Foxp represses the expression of a key component of adherens junctions, N-cadherin, and promotes the detachment of differentiating neurons from the neuroepithelium. Conversely, inactivation of Foxp2 and Foxp4 function in both chick and mouse results in a spectrum of neural tube defects associated with neuroepithelial disorganization and enhanced progenitor maintenance. Together, these data reveal a Foxp-based transcriptional mechanism that regulates the integrity and cytoarchitecture of neuroepithelial progenitors.

INTRODUCTION

The development of the central nervous system (CNS) depends upon the ability of dividing neural stem and progenitor cells (NPCs) to produce an array of neurons and glia that carry out specialized functions in mature neural networks. An essential feature of NPCs is their ability to balance self-renewal with differentiation; the progenitor population must initially expand in numbers yet then cease dividing to form specific cell types at appropriate times and places in the embryo. Disruptions in this balance contribute to neurodevelopmental abnormalities that can affect the gross size and organization of the nervous system (Pang et al., 2008) or impair cognitive and motor functions (Courchesne et al., 2007). An important step toward understanding the basis of these defects thus lies in defining the gene regulatory pathways that regulate NPC renewal.

Throughout development, NPCs are organized in a polarized neuroepithelial sheet that surrounds the ventricles, termed the ventricular zone (VZ). This arrangement fosters progenitor-progenitor contacts that serve as a self-supporting neural stem cell niche (Zhang et al., 2010). Within this compartment, NPCs exhibit a characteristic bipolar radial morphology mediated by two points of adhesion. At their apical pole, NPCs adhere to the luminal surface of the ventricle through N-cadherin-based adherens junctions (AJs) formed between neighboring NPCs, while their basal end-feet are attached to the subpial extracellular matrix through integrin-laminin interactions (Meng and Takeichi, 2009). AJs maintain the radial morphology and self-renewal of NPCs by anchoring a variety of signaling proteins to the actin cytoskeleton. Some of the best studied of these factors include the following: (1) members of the catenin/armadillo protein family (α, δ, γ, and β-catenin, the latter of which also mediates the proliferative activity of the Wnt signaling pathway) (Farkas and Huttner, 2008; Meng and Takeichi, 2009; Stepniak et al., 2009); (2) Par proteins, aPKC, and Cdc42, which control apical-basal polarity (Cappello et al., 2006; Manabe et al., 2002; Sottocornola et al., 2010); and (3) Numb, an asymmetrically distributed regulator of Notch pathway activity and neuronal differentiation (Cayouette and Raff, 2002; Rasin et al., 2007).

Most studies of AJs in NPCs have focused on how these signaling complexes are assembled to sustain the neuroepithelial state. However, a less understood, but equally important aspect is the means by which AJs are disassembled to permit NPC differentiation and migration away from the VZ. This process must be tightly regulated, as blocking the expression or activity of AJ components causes NPCs to delaminate,

resulting in widespread disruption of the neuroepithelium and deformation of the neural tube (Cappello et al., 2006; Chen et al., 2006; Ghosh et al., 2008; Imai et al., 2006; Kadowaki et al., 2007; Rasin et al., 2007; Zechner et al., 2003; Zhang et al., 2010).

To study this critical step in neurogenesis, we have focused on the formation of motor neurons (MNs) in the spinal cord. MN progenitors are specified at an early stage in development through the convergent actions of Sonic hedgehog and retinoic acid signaling, which direct a network of transcription factors centered around the bHLH protein Olig2 to promote MN differentiation (Briscoe and Novitch, 2008). In our efforts to identify transcription factors that are deregulated in *Olig2* mutant mice, we found that two Forkhead domain proteins, Foxp1 and Foxp4, are highly associated with MN formation and showed that Foxp1 is essential for the subtype identity and migratory behavior of differentiated MNs (see Figures S1A and S1B available online; Palmesino et al., 2010; Rousso et al., 2008). In subsequent analyses, we observed that Foxp4 and a related protein, Foxp2, are expressed well before the onset of Foxp1, and Foxp4 appearance notably coincides with the initiation of MN differentiation and emigration of neurons from the VZ neuroepithelium (Figure S1). This striking pattern led us to consider that Foxp2 and Foxp4 might play important roles in regulating cell adhesion during MN formation.

Foxp proteins are transcriptional repressors expressed in many tissues, and their individual and cooperative functions are essential for blood, heart, lung, and gut development (Hu et al., 2006; Li et al., 2004a, 2004b; Lu et al., 2002; Shu et al., 2007; Wang et al., 2004). Foxp1, Foxp2, and Foxp4 exhibit both overlapping and region-specific patterns within the developing spinal cord and forebrain (Dasen et al., 2008; Ferland et al., 2003; Rousso et al., 2008; Takahashi et al., 2003, 2008; Tamura et al., 2003, 2004), and their mutation has been linked to cognitive disorders that affect language acquisition such as autism (Groszer et al., 2008; Lai et al., 2001; O'Roak et al., 2011; Shu et al., 2005), as well as defects in MN fate selection and movement disorders (Dasen et al., 2008; Pariani et al., 2009; Rousso et al., 2008; Sürmeli et al., 2011). While clearly important for neural development, the molecular functions of Foxp proteins remain poorly defined.

In this study, we identify a role for Foxp2 and Foxp4 in regulating the cytoarchitecture of neuroepithelial progenitors. Both proteins are upregulated upon neuronal differentiation in the spinal cord and brain, and Foxp4 elevation coincides with a downregulation of N-cadherin expression and detachment of NPCs from the neuroepithelium. When misexpressed, Foxp proteins potently suppress N-cadherin expression, resulting in a loss of AJs and ectopic neurogenesis. In contrast, inactivation of Foxp2 and Foxp4 function impairs NPC differentiation and exit from the neuroepithelium, resulting in a variety of neural tube defects. These suppressive actions of Foxp proteins act in opposition to the NPC determinant Sox2, which promotes N-cadherin expression and maintains cells in an undifferentiated state. Together, these data identify Foxp2 and Foxp4 as critical components of a transcription factor network that regulates the integrity and self-renewal of NPCs throughout the CNS.

RESULTS

Foxp4 Elevation Coincides with MN Differentiation and Neuroepithelial Detachment

To assess the function of Foxp proteins in neurogenesis, we first mapped their expression in the chick spinal cord during the peak period of MN progenitor formation and differentiation, embryonic day (e)2–e5 (Figures 1 and S1). Foxp2 was associated with all spinal cord NPCs from e2 onward, whereas Foxp4 appeared slightly later in subsets of NPCs with a notable enrichment in Olig2$^+$ MN progenitors (pMN) (Figures 1A, 1B, 1D, 1E, S1C–S1J, and S1O–S1R). Foxp4 increased as the pMN began to differentiate, but was extinguished from most Isl1/2$^+$ MNs (Figures 1B, 1D, and 1E). Foxp1, in comparison, was confined to postmitotic MNs (Figure 1C and S1K–S1N). The successive expression of Foxp2, Foxp4, and Foxp1 was also evident in the mouse spinal cord (Figures 1R–1V), suggesting that this is a conserved feature of vertebrate MN development.

Within the pMN, the graded expression of Foxp4 demarcated different stages of MN development: Foxp2 and low levels of Foxp4 (Foxp4^{low}) were present in Sox2$^+$ Olig2$^+$ MN progenitors in the VZ, while Foxp2 and ~2-fold higher levels of Foxp4 (Foxp4^{high}) were associated with differentiated cells in the intermediate zone (IZ) (Figures 1B, 1E, 1F, 1M, and 1Q). Most Foxp4^{high} cells expressed the proneural transcription factors Ngn2 and NeuroM and displayed cytoplasmic accumulation of Numb protein (Figures 1G–1I). Foxp2 and Foxp4 were both downregulated as MNs entered the mantle zone (MZ) marked by NeuN and Isl1/2 staining (Figures 1E, 1J, 1K, and S1C–S1R).

We next used intraventricular injections of horseradish peroxidase (HRP) to identify apically adhered neuroepithelial progenitors and bromodeoxyuridine (BrdU) labeling to measure their proliferation (Figure 1L). Cells with a Foxp2$^+$ Foxp4^{low} status comprised cycling HRP$^+$ BrdU$^+$ neuroepithelial progenitors, whereas Foxp2$^+$ Foxp4^{high} cells were detached and postmitotic (HRP$^-$ BrdU$^-$; Figures 1M–1O and 1Q). In contrast, injections of rhodamine-dextran into the ventral roots of the spinal cord marked Foxp2^{off} Foxp4^{off} mature MNs that lacked apical processes (Figure 1P). Foxp4 elevation thus coincides with the delamination of newborn MNs from the VZ and is shut off as these cells migrate into the MZ and extend axons (Figure 1W).

Foxp Activity Is Necessary and Sufficient to Promote Neuronal Differentiation and Detachment from the Neuroepithelium

To test whether Foxp4 elevation could promote neuronal differentiation, we used in ovo electroporation to unilaterally express Foxp4 along with an IRES-nuclear EGFP (nEGFP) reporter in the e3 chick spinal cord. The effects of these manipulations on progenitor maintenance, cell migration, and neural tube cytoarchitecture were monitored 8–36 hr later in comparison to electroporation with an empty IRES-nEGFP vector. Foxp4 misexpression led to extensive delamination of cells from the ventral neuroepithelium, resulting in a depletion of Sox2$^+$ Olig2$^+$ MN progenitors and accumulation of transfected cells within the VZ and luminal space (Figures 2A–2G). These clusters contained NeuN$^+$ neurons expressing Isl1, Isl2, Hb9, and other MN markers along with some Chx10$^+$, Gata3$^+$, and Evx1$^+$ interneurons

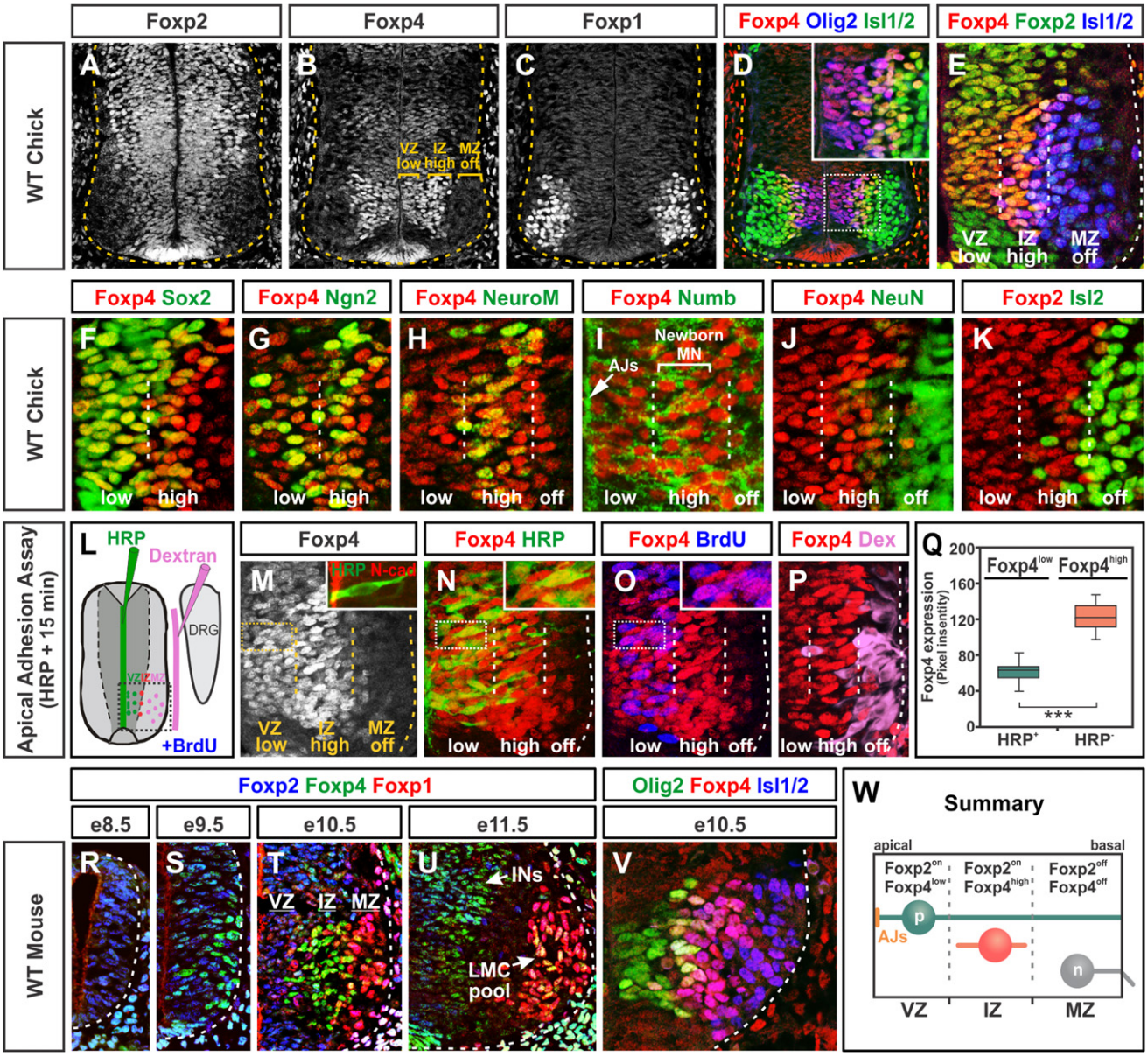

Figure 1. Elevated Foxp4 Expression Coincides with Neuronal Differentiation and Neuroepithelial Detachment

(A–E) Foxp2, Foxp4, and Foxp1 are successively expressed by differentiating MN progenitors and other spinal NPCs. Foxp4 levels increase during this transition.

(F–K) Foxp4^{low} cells express Sox2; Foxp4^{high} cells express the proneural proteins Ngn2 and NeuroM, and display cytoplasmically localized Numb. Foxp2 and Foxp4 are absent from mature NeuN^{+} Isl2^{+} MNs.

(L–P) Neuroepithelial attachment, cell cycle exit, and neuronal maturation are distinguished by HRP injections into the ventricle, rhodamine-dextran injections into the ventral roots, and BrdU labeling.

(Q) Quantification of Foxp4 levels in HRP^{+} (neuroepithelial) and HRP^{-} (detached) cells. Mean pixel intensities ± SEM calculated from at least 25 cells per group from multiple embryos are shown. ***$p < 0.001$.

(R–V) The sequential pattern of Foxp expression is conserved in the mouse spinal cord. (U) At e11.5, Foxp4 is also observed in a putative LMC motor pool, and in numerous interneurons (INs).

(W) Summary of Foxp4 and Foxp2 expression during MN differentiation. AJs, adherens junctions.

See also Figure S1.

(Figures 2C–2G, S2A, S2B, S2D, S2E, S2G, S2H, and data not shown). While most of the mispositioned cells contained the GFP transfection marker, nontransfected neurons were also present in these clusters suggesting that Foxp4 elevation leads to both cell-autonomous and nonautonomous changes in neuronal differentiation and/or lateral migration. Ectopic neurons were similarly seen with the misexpression of Foxp2 and Foxp1, but these effects were distinct from the misexpression of other

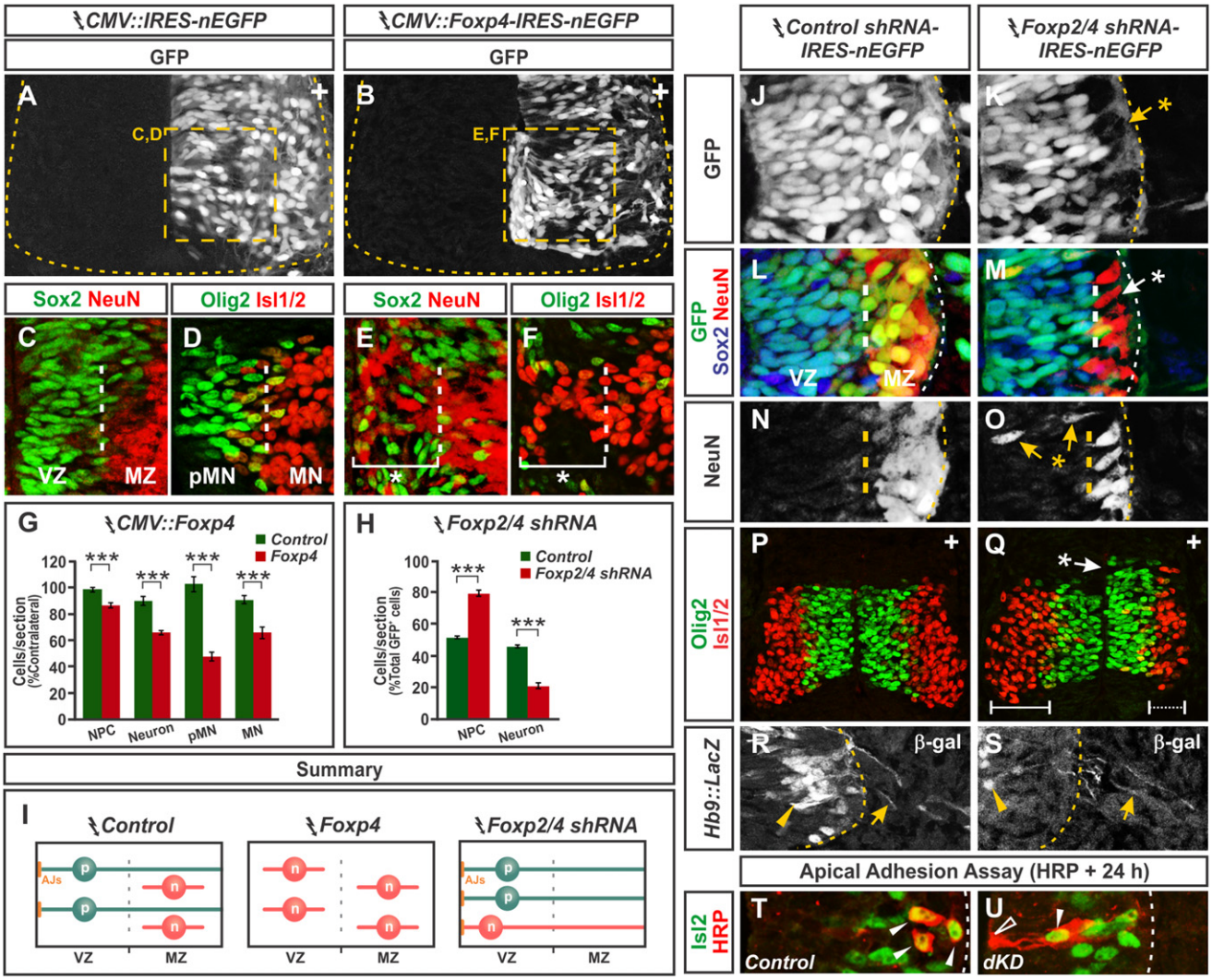

Figure 2. Foxp2 and Foxp4 Promote Neurogenesis and Suppress Neuroepithelial Character

(A, C, and D) Analysis of spinal cords transfected with *CMV::IRES-nEGFP*-control or (B, E, and F) *CMV::Foxp4-IRES-nEGFP* expression vectors. Brackets with asterisks indicate areas of ectopic neurogenesis.

(G and H) Quantification of changes in neurogenesis. NPC, $Sox2^+$; Neuron, $NeuN^+$; pMN, $Olig2^+$; MN, $Isl1/2^+$. Mean ± SEM from multiple sections taken from 5 embryos for each condition are shown. ***$p < 0.001$.

(J–U) Analysis of spinal cords transfected with *Foxp2* and *Foxp4 shRNA-IRES-nEGFP* vectors or a nontargeting control *shRNA-IRES-nEGFP* vector. Most double-knockdown (dKD) cells express Sox2 and do not form $NeuN^+$ neurons (asterisk in K and M). Some dKD cells differentiate within the neuroepithelium (arrows in O). Asterisk in (Q) indicates a dorsal expansion of $Olig2^+$ MN progenitors; brackets denote a decrease in MNs. (R and S) *Foxp2/4* dKD MNs extend *Hb9::LacZ*$^+$ axons toward the periphery (arrows), but their cell bodies fail to migrate laterally (arrowheads). (T and U) *Foxp2/4* dKD MNs retain apical attachments (open arrowhead) and radial morphology. (I) Summary of the effects of Foxp2 and Foxp4 manipulation on neurogenesis and apical attachment.

See also Figures S2, S3, and S4.

proteins known to promote neurogenesis including Ngn2 and the cyclin-dependent kinase inhibitor $p27^{Kip1}$ (Figure S3). These latter agents caused transfected cells to rapidly exit the cell cycle, differentiate, and migrate laterally without any significant disturbance to the neuroepithelium.

We next assessed the endogenous functions of Foxp2 and Foxp4 in the chick spinal cord using short hairpin RNA (shRNA) vectors carrying an IRES-nEGFP reporter to knock down Foxp2 and Foxp4 expression individually and in combination (Figure S4). While Foxp2 knockdown alone had little effect, Foxp4 knockdown alone and more notably in combination with Foxp2 loss trapped most of the transfected cells within the VZ and prevented their migration into the MZ (Figures 2J, 2K, S4A–S4D, and S4U–S4X). Greater than 80% of the Foxp2/4 shRNA-transfected cells expressed progenitor markers such as Sox2 and Olig2 compared to ~55% in control samples (Figures 2H, 2L, 2M, 2P, and 2Q). The formation of neurons was accordingly reduced with ~20% of cells transfected with Foxp2/4 shRNAs expressing NeuN compared to ~50% in the controls (Figures 2H and 2L–2Q). Consequently, the width of

the MZ was thinner on the shRNA-transfected side of the spinal cord (Figures 2L–2O). While MN loss was most obvious, interneuron formation was also suppressed by these manipulations (Figures S2C, S2F, and S2I). Interestingly, in cases where the Foxp2/4 shRNA transfected cells had differentiated, these neurons were abnormally retained within the VZ (Figures S4U–S4X), suggesting that the loss of Foxp2 and Foxp4 might have impaired their ability to detach from the neuroepithelium or migrate to the MZ.

To address whether these defects were due to abnormal neuroepithelial adhesion, we labeled apically attached cells with HRP injections and monitored their fate after 24 hr of development. In control embryos, most HRP-labeled cells migrated laterally to colonize the ventral horns and expressed mature MN markers such as Isl2 and a cotransfected Hb9::LacZ reporter (Figures 2R and 2T). In contrast, HRP-labeled MNs transfected with Foxp2/4 shRNAs remained medially positioned in the VZ and inappropriately maintained apical contacts with the neuroepithelium (Figures 2S and 2U). Despite these defects, MNs lacking Foxp2 and Foxp4 still expressed Isl2 and projected Hb9::LacZ$^+$ axons through the ventral roots (Figures 2S and 2U). Thus, Foxp2 and Foxp4 loss uncouples the processes of neuroepithelial detachment, lateral migration, and axon extension. Taken together, these results indicate that Foxp activities are both necessary and sufficient to promote neuroepithelial detachment and differentiation in the developing spinal cord (Figure 2I).

Foxp Proteins Repress N-Cadherin and Disrupt Adherens Junctions

The structural integrity of the neuroepithelium and maintenance of NPCs depends on homophilic interactions between N-cadherin proteins present in AJs formed between neighboring cells (Farkas and Huttner, 2008; Meng and Takeichi, 2009; Stepniak et al., 2009). Given that these adhesive contacts must be shed upon differentiation, we next investigated whether the pro-differentiation actions of Foxp4 might involve changes in N-cadherin expression or subcellular distribution. In transverse sections of the spinal cord, we noticed that there was a slight thinning of apical N-cadherin staining around the region of the pMN (Figure 3A, bracket). This difference was more clearly revealed by imaging the apical surface of the neuroepithelium in an open book preparation, which showed distinct bands of N-cadherin staining corresponding to the different progenitor domains along the dorsoventral axis (Figures 3B–3E and S5A–S5J). N-cadherin was strikingly reduced wherever Foxp4 was present (Figures 3B and 3D–3F; averaged correlation R^2 = −0.722). This antithetical pattern was specific to Foxp4 and N-cadherin as there was no correlation between the expression of Foxp4 and other AJ components such as aPKCζ or the NPC marker Sox2 (Figures 3B, 3C, and S5B–S5L).

Under conditions of Foxp4 misexpression, the electroporated spinal cords displayed a dramatic loss of N-cadherin protein and disruption in the ultrastructure of the neuroepithelium (Figures 3G, 3K, 3M, and 3Q). These changes coincided with an aberrant distribution or loss of other AJ components including β-catenin, f-actin, aPKCζ, and Par3 (Figures 3H, 3I, 3N, and 3O, and data not shown) and cytoplasmic accumulation of Numb (Figures 3L, 3M, and 3R). The radial morphology of NPCs was also severely disrupted (Figures 3H, 3I, 3N, and 3O), and markers of dividing cells such as BrdU incorporation and phosphohistone H3 staining were reduced (data not shown). Nonetheless, integrin-laminin interactions at the basolateral membrane remained intact (Figures 3J and 3P), suggesting that the effects of Foxp4 misexpression are primarily directed to apical attachments. Identical results were seen with misexpression of Foxp2 and Foxp1 (Figure S3), indicating that all of the Foxp proteins have the capacity to repress N-cadherin expression and disrupt AJs under these conditions.

The combined knockdown of Foxp2 and Foxp4, in contrast, led to an ~1.5–2-fold upregulation of N-cadherin mRNA and protein within the pMN and extensive accumulation of Numb at the apical membrane of these cells (Figures 3S, 3T, and S5M–S5Q). The effects of the shRNA constructs were specific, as the knockdown phenotype was completely reversed by coelectroporation of a Foxp4 expression vector, often resulting in the Foxp4 misexpression phenotype (Figures S2J–S2R). Together, these data indicate that Foxp2 and Foxp4 play a crucial role suppressing the expression of N-cadherin and disassembling neuroepithelial AJs (Figure 3U).

N-Cadherin Is a Direct Target of Foxp4

To determine whether N-cadherin is a direct target of Foxp4 or is repressed as a secondary effect of cells undergoing neurogenesis, we assessed the order of events leading up to the ectopic appearance of neurons in the VZ following Foxp4 misexpression and measured corresponding changes in mRNA expression. The first clear defect was a decrease in N-cadherin staining starting around 12 hr posttransfection, followed thereafter by a loss of Sox2 staining and cytoplasmic accumulation of Numb at 24 hr posttransfection, and the ectopic formation of NeuN$^+$ neurons within the VZ by 36 hr posttransfection (Figures 4A–4O). We did not observe any notable elevation of either Ngn2 or NeuroM above that already present in the spinal cord during this time course (data not shown), suggesting that the prodifferentiation actions of Foxp4 work downstream or in parallel with endogenous proneural gene activity.

We next FACS-isolated transfected cells from the electroporated spinal cords and measured mRNA expression levels using quantitative PCR. Foxp4 misexpression resulted in an ~45% decrease in *N-cadherin* mRNA within 6 hr and an ~65% decrease by 12 hr postelectroporation (Figure 4P). We did not observe any significant decrease in the expression of other AJ genes such as *β-catenin*, *Cdc42*, *RhoA*, and *aPKCζ* at the 6 hr time point, though *β-catenin* mRNA was moderately reduced by 12 hr postelectroporation (Figure 4P). Despite this latent *β-catenin* reduction, we did not detect any changes in β-catenin activity as measured by a cotransfected Wnt/β-catenin-responsive reporter, TOP-dGFP (Dorsky et al., 2002), or find any correlation between reporter expression and the endogenous pattern of Foxp4 expression (Figures S2S–S2V). These results suggest that the decline in *β-catenin* levels may be secondary to N-cadherin loss.

In evaluating the expression of other genes, we found that Foxp4 potently suppressed *Sox2* mRNA by ~70% within 6 hr postelectroporation (Figure 4P). Despite this early transcriptional

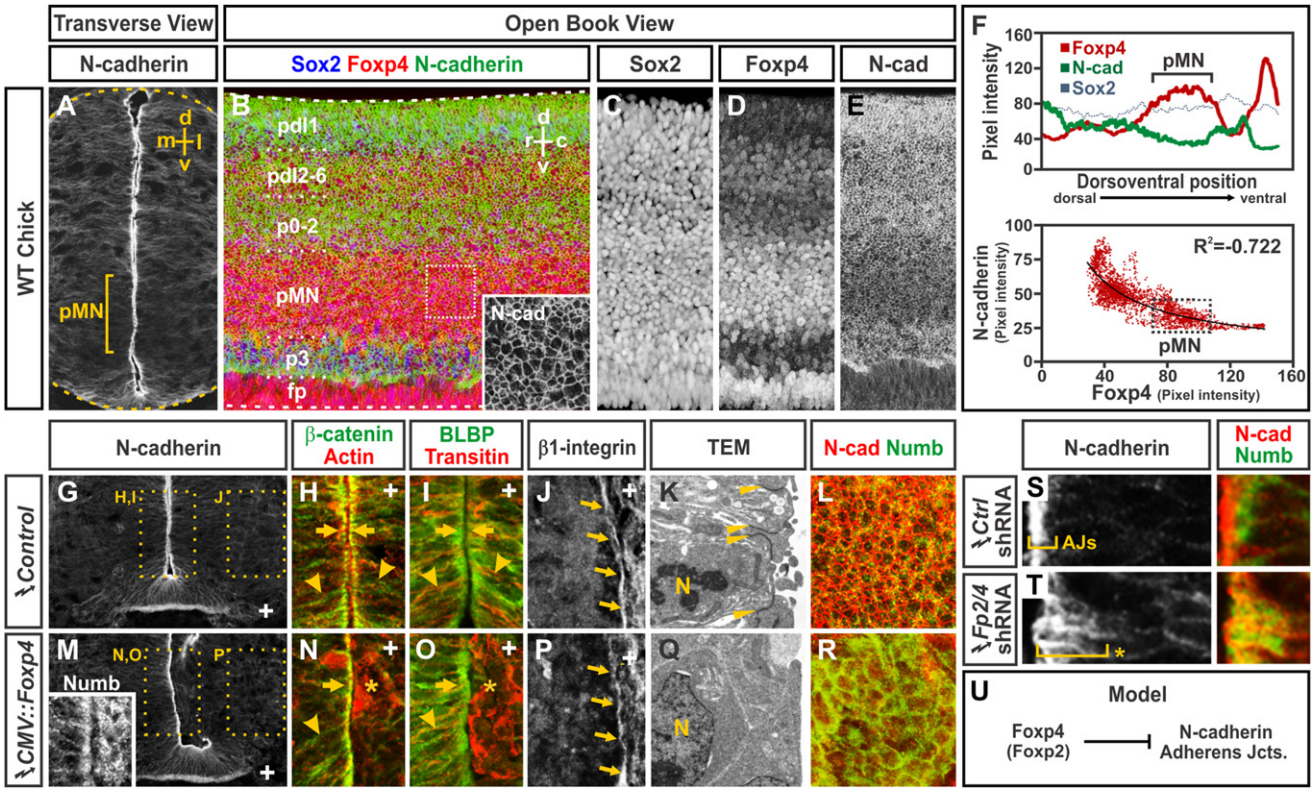

Figure 3. Foxp4 Represses N-Cadherin and Influences Adherens Junction Ultrastructure

(A–E) Transverse and open book views of the spinal cord reveal differential expression of Foxp4 and N-cadherin in distinct progenitor (p) domains. d, dorsal; v, ventral; m, medial; l, lateral; r, rostral; c, caudal.

(F) N-cadherin and Foxp4 expression are inversely correlated [$f(x) \propto x^{-0.75}$, $R^2 = -0.722$].

(G–R) Analysis of spinal cords transfected with (G-L) *CMV::IRES-nEGFP*-control or (M-R) *CMV::Foxp4-IRES-nEGFP* vectors. + indicates the transfected side of the spinal cord. Arrows and arrowheads indicate apical membranes and radial processes, respectively. Asterisks denote disruptions in neuroepithelial cytoarchitecture. Arrows in (J) and (P) indicate the intact pial surface.

(K and Q) Transmission electron micrograph of normal (arrowheads) and disrupted AJs. N, nucleus.

(L and R) Open book view of Numb anchored to the apical membrane and its redistribution after Foxp4 misexpression.

(S and T) N-cadherin and Numb accumulate at the apical surface of the neuroepithelium upon Foxp2/4 double knockdown.

(U) Summary of the suppressive effects of Foxp4 and Foxp2 on N-cadherin and AJ maintenance.

See also Figures S2, S3, S4, and S5.

effect, Sox2 protein did not decline until ~18–24 hr postelectroporation, at which time N-cadherin was undetectable (Figures 4A, 4B, 4F, and 4G). Together, these data indicate that Foxp4 can rapidly suppress both *N-cadherin* and *Sox2* mRNA expression, but N-cadherin protein is more labile such that it declines before Sox2 and thus initiates the process of neuroepithelial detachment.

To confirm that Foxp4 directly regulates *N-cadherin*, we aligned the genomic sequence of the chick, mouse, and human *Cdh2* (*N-cadherin*) loci and identified several evolutionarily conserved regions within introns 2 and 3 that contained canonical Foxp binding sites (Figures 4Q and S6A–S6G). Foxp4 binding to these elements was measured through chromatin immunoprecipitation assays using differentiating MN progenitors produced in vitro from mouse embryonic stem cells as a proxy for spinal cord tissue. Foxp4 binding was prominent at a highly conserved element within intron 3 [i3a] but not at other sites tested (Figures 4Q and S6). The level of Foxp4 binding to the [i3a] element was comparable to Sox2 binding to a previously identified element in the second intron of *Cdh2* [i2a] associated with N-cadherin activation (Figure 4Q; Matsumata et al., 2005). Collectively, these results provide evidence that N-cadherin expression and neuroepithelial maintenance are controlled by both activating inputs provided by Sox2 and repressive inputs provided by Foxp4, mediated by distinct enhancer elements.

Opponent Actions of Foxp4 and Sox2 Set the Level of N-Cadherin Expression to Regulate Progenitor Maintenance

If N-cadherin is the critical target for Foxp repression, then the same ectopic differentiation phenotype should be observed by directly blocking N-cadherin activity. To this end, we misexpressed a dominant-negative form of N-cadherin (dn-N-Cad) lacking its extracellular domain, which disrupts adhesions between neighboring cells (Tanabe et al., 2006). High levels of dn-N-cad disrupted the radial structure of the neuroepithelium,

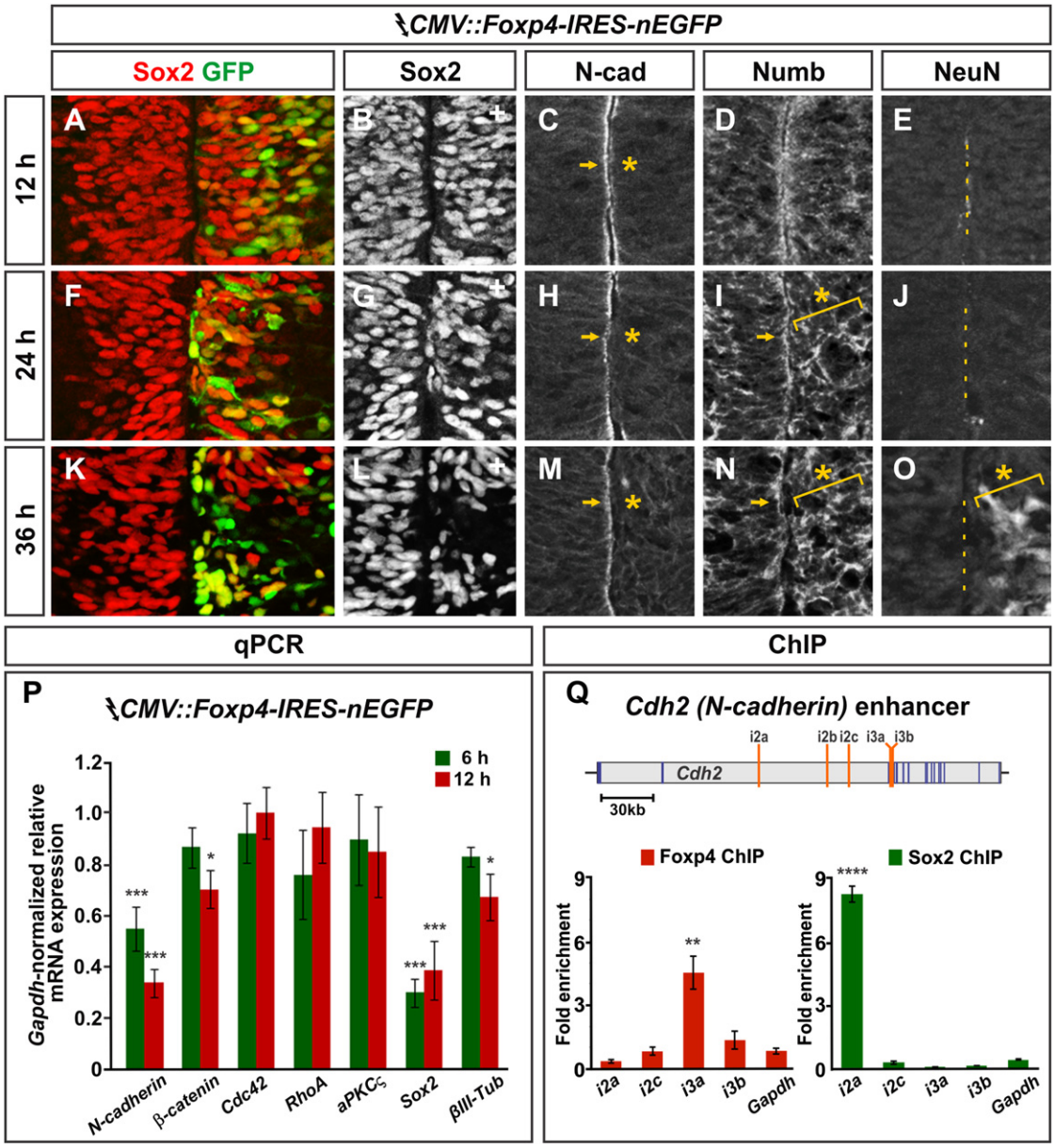

Figure 4. N-Cadherin Is a Primary Target of Foxp4

(A–O) Analysis of spinal cords transfected at e3 with a *CMV::Foxp4-IRES-nEGFP* expression vector and collected 12, 24, and 36 hr later. N-cadherin protein declines (asterisk) between 12 and 24 hr posttransfection while Sox2 perdures. By 24 hr, Numb accumulates in the cytoplasm (bracket). At ≥ 36 hr, Sox2 is abolished and cytoplasmic Numb is associated with ectopic NeuN$^+$ neurons.

(P) Quantitative PCR analysis of gene expression 6 and 12 hr after *Foxp4* transfection relative to control electroporations. Mean *Gapdh*-normalized mRNA expression levels ± SEM from at least 3 embryos per condition are shown. *$p < 0.05$; ***$p < 0.001$.

(Q) Chromatin immunoprecipitation analysis of Foxp4 and Sox2 at evolutionarily conserved regions of the *Cdh2* (*N-cadherin*) locus indicated by the orange lines. Foxp4 shows significant binding to an element in intron 3 [i3a] relative to other regions in the *Cdh2* locus and unrelated genes such as *Gapdh*. Sox2 binds to an element in intron 2 [i2a] but not to regions where Foxp4 is bound. Mean binding activity ± SEM from four experiments is plotted. **$p < 0.01$; ****$p < 0.0001$.

See also Figure S6.

resulting in a cytoplasmic accumulation of Numb and ectopic formation of NeuN$^+$ neurons in the VZ much like the defects seen after Foxp4 misexpression (Figures 5A, 5B, 5F, 5G, 5K, 5L, 5P, 5Q, 5U, 5V, 5Z, and 5AC). Interestingly, low-level misexpression of dn-N-cad also promoted neuronal differentiation, but under these conditions AJs and the radial structure of the neuroepithelium was preserved. The majority of these transfected cells settled in the IZ, though they rarely migrated further into the MZ (Figures 5C, 5H, 5M, 5R, 5W). Misexpression of full-length N-cadherin had the opposite effect, retaining most of

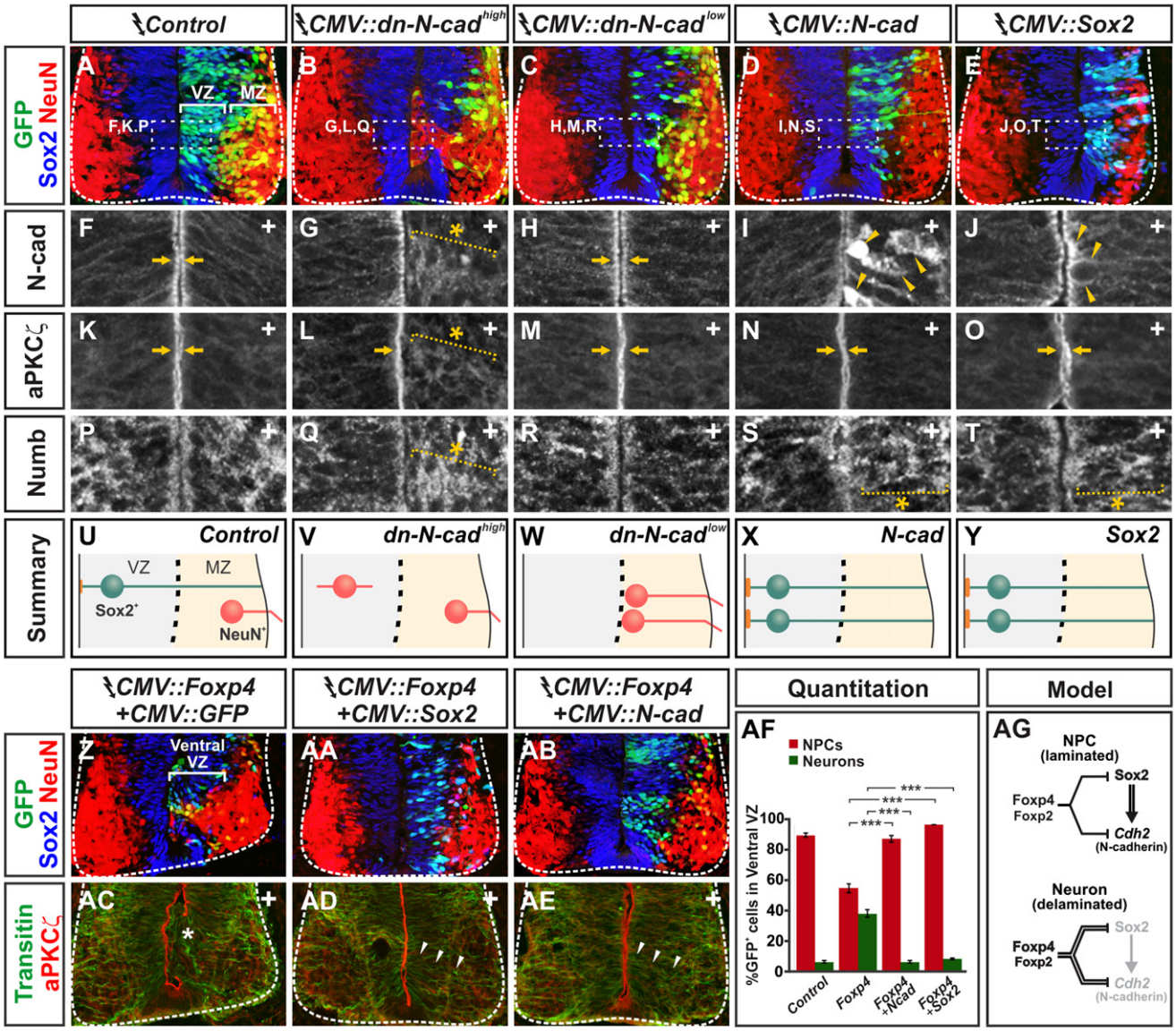

Figure 5. Sox2 and N-Cadherin Promote Neuroepithelial Character and Oppose Foxp4 Function

(A, F, K, and P) Analysis of spinal cords transfected with a *CMV::IRES-nEGFP* control vector compared to equivalent vectors encoding: (B, G, L, and Q) dominant-negative *N-cadherin* at high (*dnN-cad*^{high}) or (C, H, M, and R) low (*dnN-cad*^{low}) dosage; (D, I, N, and S) full-length *N-cadherin*; (E, J, O, and T) *Sox2*. Most cells transfected with *dnN-cad*^{high} or *dnN-cad*^{low} express NeuN and lack neuroepithelial characteristics. Full-length *N-cadherin* maintains cells in an NPC-like state within the VZ (D), similar to *Sox2* (E). Arrows and brackets with asterisks denote the normal and altered distribution of proteins, respectively. + indicates the transfected side of the spinal cord.

(U–Y) Summaries of the effects of manipulating N-cadherin or Sox2 on neurogenesis and apical attachment.

(Z–AE) Cotransfection of *Foxp4* with full-length *N-cadherin* or *Sox2* restores neuroepithelial character. Asterisk in (AC) indicates region of Foxp4-induced neuroepithelial disruption. Arrowheads in (AD)–(AE) indicate restoration of radial fibers.

(AF) Quantitation of Sox2$^+$ NPCs and NeuN$^+$ neurons in the ventral VZ under the indicated conditions. Plots show mean ± SEM from multiple sections collected from 3–5 embryos for each condition. ***$p < 0.001$.

(AG) Summary of the opposing actions of Foxp4 and Sox2 in regulating N-cadherin expression and progenitor maintenance.

the transfected cells in a progenitor-like state within the VZ (Figures 5D, 5I, 5N, 5S, and 5X).

Sox2 is known to activate N-cadherin expression in many regions of the CNS, and its elevation can block neuronal differentiation (Bylund et al., 2003; Graham et al., 2003; Matsumata et al., 2005). We therefore examined whether Sox2 misexpression could increase N-cadherin and thereby offset the progenitor-suppressing actions of Foxp4. When Sox2 was elevated, apical staining for N-cadherin and other components of AJs such as aPKCζ and Numb was increased, reminiscent of the

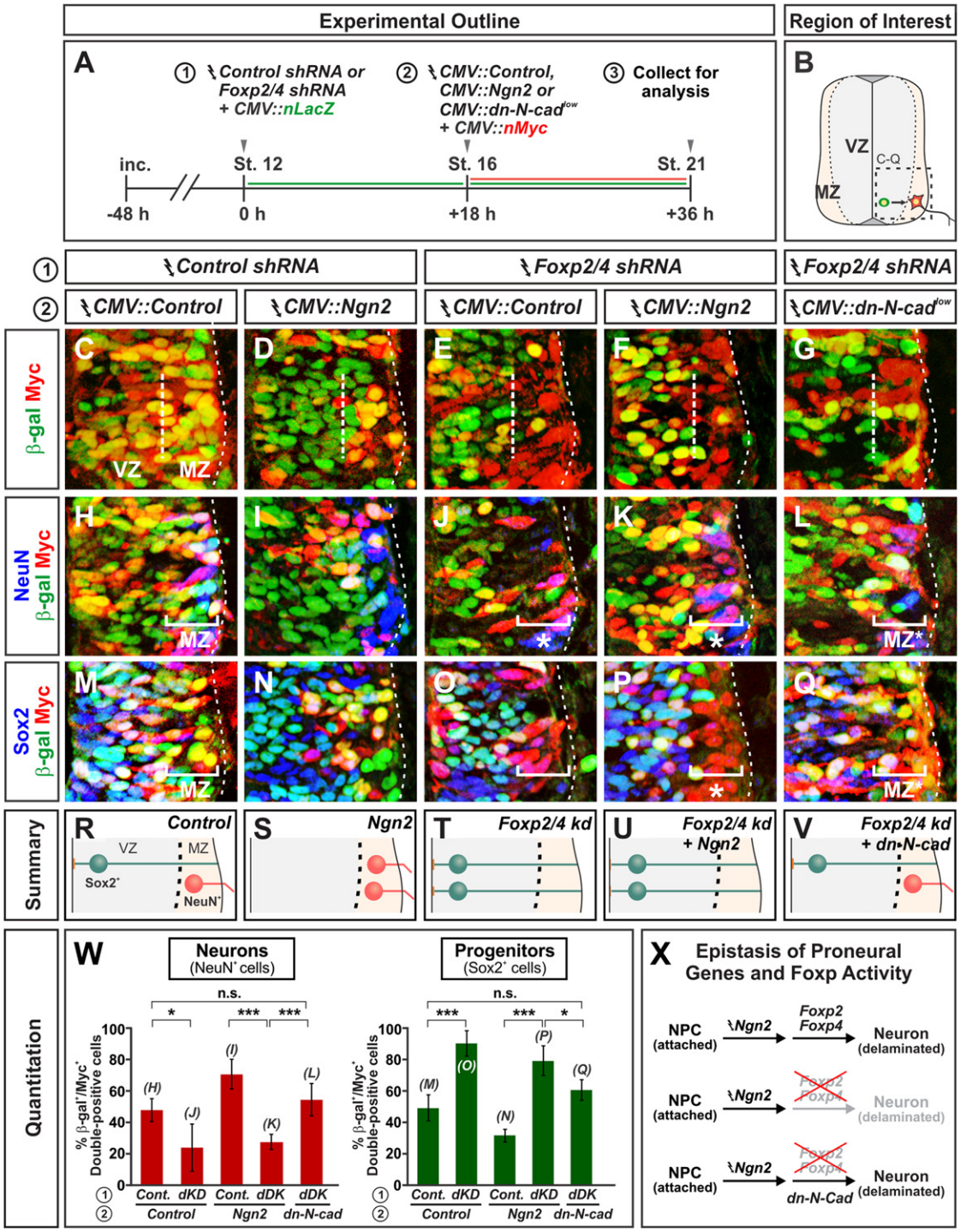

Figure 6. Proneural Gene Activity Requires Foxp2/4 Function to Promote Neurogenesis

(A) Outline of the double transfection protocol. *CMV::nuclear-tagged LacZ (nLacZ)* and *CMV::nuclear Myc-tags (nMyc)* distinguish the first and second transfections, respectively.

(B) Model of the neural tube showing the region analyzed. Costaining with β-gal, Myc, and markers for $Sox2^+$ NPCs or $NeuN^+$ neurons results in "white" triple-labeled cells in (H)–(Q).

(C, H, and M) Cells doubly transfected with control vectors comprise NPCs and neurons equally.

(D, I, and N) Cells doubly transfected with control vectors followed by Ngn2 predominantly form neurons in the MZ.

Cells doubly transfected with *Foxp2/4* shRNA followed by control (E, J, and O) or Ngn2 vectors (F, K, and P) do not form neurons and remain in the VZ.

(G, L, and Q) Cells doubly transfected with *Foxp2/4* shRNA followed by low amounts of the dnN-cad vector detach and differentiate.

phenotype seen with Foxp2 and Foxp4 knockdown (compare results in Figures 3S and 3T to Figures 5E, 5J, 5O, 5T, and 5Y). Moreover, the majority of transfected cells remained in the VZ and neuronal differentiation was blocked (Figures 5A and 5E). When Sox2 was coexpressed with Foxp4, N-cadherin levels and AJs were fully restored and cells were held in a NPC state (Figures 5Z–5AA, 5AC, 5AD, and 5AF). Identical results were obtained with the coexpression of Foxp4 with full-length N-cadherin (Figures 5AB, 5AE, 5AF). Thus, Foxp4 appears to work in opposition to Sox2 in setting the level of N-cadherin expression to balance progenitor maintenance with differentiation (Figure 5AG).

Foxp2 and Foxp4 Act Downstream of Proneural Genes and Are Required for Their Differentiation-Promoting Functions

We next set out to determine where Foxp4 functions in the neurogenic cascade that mediates neuronal differentiation. In the normal course of MN development, Foxp4 elevation coincided with the onset of Ngn2 and NeuroM expression (Figures 1G and 1H), suggesting that it might act downstream of proneural gene activity. To explore this relationship, we examined spinal cords in which the Notch effector Hes5-2 had been misexpressed. Hes5-2 potently suppressed Ngn2 expression and the formation of $p27^{Kip1+}$ neurons, and maintained cells in a progenitor state (Figure S7). Under these conditions, Foxp4 levels were significantly reduced (Figures S7G and S7J), indicating that proneural gene activity is required for Foxp4 expression.

To investigate the epistatic relationship between Foxp4 and proneural gene activity further, we examined whether the blockade in neuronal differentiation following Foxp2 and Foxp4 knockdown could be overcome by forcing the expression of Ngn2. For this experiment, we sequentially transfected spinal cords with vectors producing Foxp2 and Foxp4 shRNAs and a nuclear β-galactosidase reporter, followed by expression vectors for Ngn2 and a nuclear Myc tag reporter 18 hr later. The effects on neurogenesis were then evaluated after another 18 hr of development (Figures 6A and 6B). Doubly transfected cells were identified by the presence of both β-gal and Myc reporters (yellow cells in Figures 6C–6G) and scored for their expression of NeuN as a measure of neuron formation (white cells in Figures 6H–6L) and Sox2 for progenitor characteristics (white cells in Figures 6M–6Q).

Whereas ~71% of cells transfected with Ngn2 alone formed $NeuN^+$ neurons and migrated to the mantle layer, the removal of Foxp2 and Foxp4 function reduced this frequency to ~28% (Figures 6C–6F, 6H–6K, 6M–6P, 6R–6U, and 6W). In addition, the majority of Ngn2 and Foxp2/4 shRNA-cotransfected cells were trapped within the VZ where they expressed Sox2, similar to the effects of Foxp2 and Foxp4 knockdown alone. The neurogenesis defects associated with Foxp2 and Foxp4 loss were nevertheless rescued by the sequential expression of low levels of dn-N-cad (Figures 6G, 6L, 6Q, 6V, and 6W). These data together suggest that neuronal differentiation driven by proneural gene expression requires Foxp function to enable differentiating cells to detach from the neuroepithelium and lose their progenitor features (Figure 6X).

Foxp4 Mutant Mice Display Numerous Defects in Brain and Spinal Cord Development

We lastly sought to evaluate whether Foxp4 function might be similarly required in the mammalian spinal cord, as suggested by the transient expression of Foxp4 during mouse MN development (Figures 1R–1V). For this analysis, we utilized two strains of *Foxp4* mutant mice: first, a targeted replacement of the Forkhead DNA binding domain with a neomycin resistance cassette ($Foxp4^{Neo}$; Li et al., 2004b), and second, a gene trap insertion between exons 5 and 6 of the *Foxp4* gene ($Foxp4^{LacZ}$) (Figure 7A). Using antibodies raised against the amino- and carboxyl-terminal ends of Foxp4, we found that a partial Foxp4 protein was produced from the $Foxp4^{Neo}$ allele while little Foxp4 protein was produced from the $Foxp4^{LacZ}$ allele (Figures S8A–S8L), suggesting that the latter may result in a more complete disruption of *Foxp4* function. Consistent with that interpretation, we observed that $Foxp4^{LacZ/LacZ}$ homozygous mutants were underrepresented in e11.5 and older litters compared to $Foxp4^{Neo/Neo}$ mutant animals (Figure 7B; $p < 0.05$ by the exact Chi square test), indicating that the $Foxp4^{LacZ/LacZ}$ mutation results in embryonic lethality starting around e10.5. Moreover, of the $Foxp4^{LacZ/LacZ}$ animals that were recovered between e10.5 and e13.5, ~28% exhibited gross neural tube defects including exencephaly, spina bifida, and holoproscencephaly, as well as occasional notochord and floor plate duplications (Figures 7C–7E, S8Q, S8R, S8V, S8W, and data not shown). Similar abnormalities were seen in $Foxp4^{Neo/Neo}$ mutants albeit at a lower frequency (~15%) (Figures 7C–7E and S8M–S8P). $Foxp4^{Neo/LacZ}$ transheterozygotes had a survival profile that was indistinguishable from the $Foxp4^{Neo/Neo}$ mutants, but they interestingly displayed a higher frequency of neural defects (~40%) (Figure 7C and data not shown). We surmise that this increase might result from the ability of $Foxp4^{Neo/LacZ}$ mutants to escape the early lethality associated with the $Foxp4^{LacZ}$ allele, at which time neural deformities become more pronounced.

The occurrence and severity of neural defects in *Foxp4* mutants were highly variable and independent of one another, with some embryos displaying normal spinal cord development despite gross disturbances in the brain, and vice versa. The basis of this variability is currently unknown though it might reflect functional redundancy between Foxp4 and other members of the Foxp gene family such as Foxp2 as seen in the chick spinal cord or possibly differential expression and imprinting of Foxp alleles as described for the human *FOXP2* gene (Feuk et al., 2006). *Foxp2; Foxp4* double mutation resulted in early

(R–V) Summary of double transfection results.
(W) Quantification of progenitor versus neuronal fates of doubly transfected cells. Plots display mean ± SEM for 250–500 $\beta\text{-gal}^+Myc^+$ cells from multiple sections taken from at least 3 embryos for each vector combination. *$p < 0.05$; ***$p < 0.001$; n.s., not significant.
(X) Summary of relationships between proneural genes, Foxp activity, and neuroepithelial adhesion.
See also Figure S7.

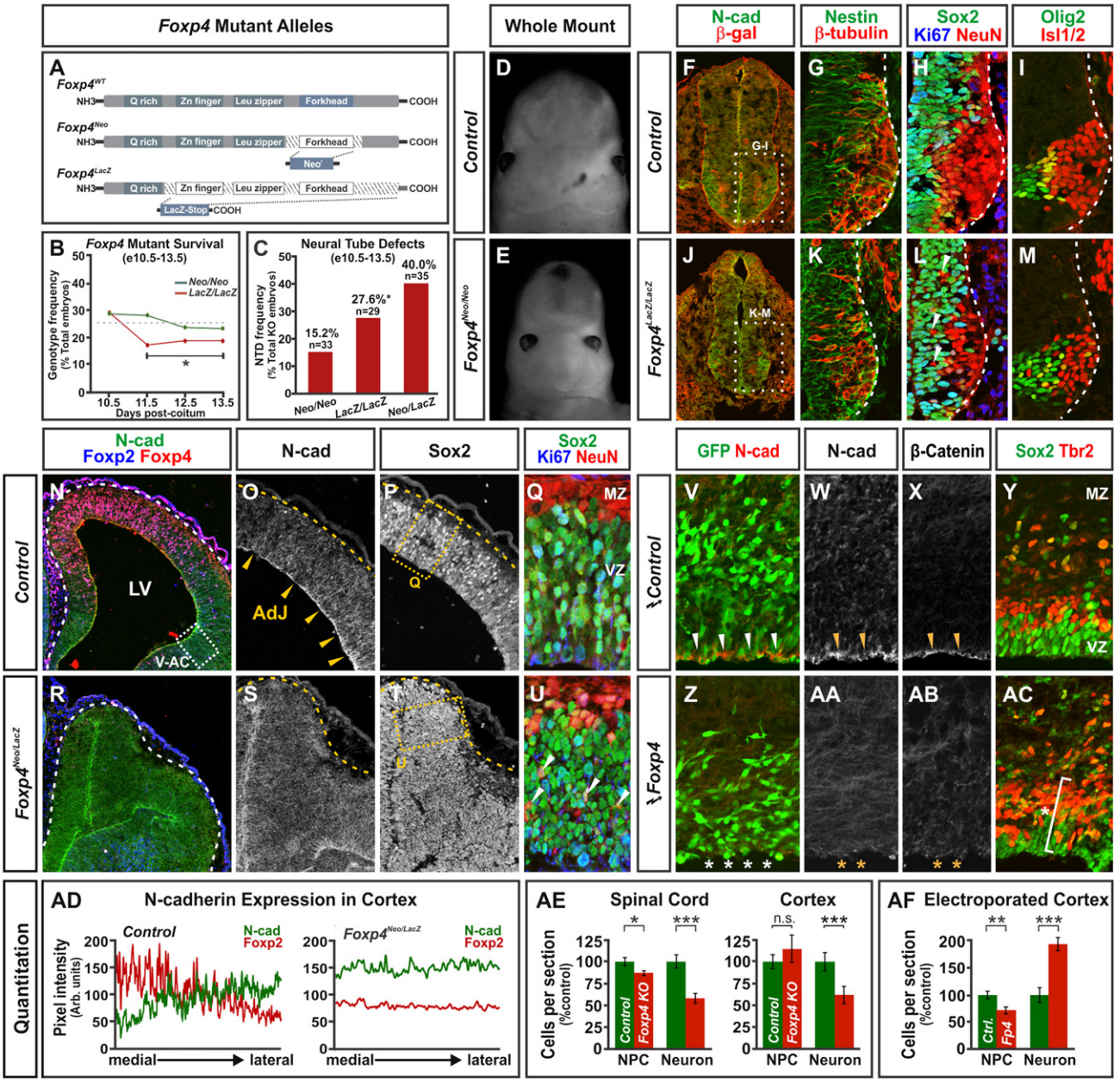

Figure 7. *Foxp4*-Deficient Mice Exhibit Defects in Neural Tube Morphology and Enhanced Progenitor Maintenance

(A) Diagram of *Foxp4* mutant alleles.

(B) Early lethality occurs by e11.5 in $Foxp4^{LacZ/LacZ}$ mutants relative to $Foxp4^{Neo/Neo}$ mice. *$p < 0.05$; $\chi^2 = 6.39$.

(C) Plot of the frequency of neural tube defects (NTD) seen in *Foxp4* mutant embryos.

(D and E) Example of intermediate holoprosencephaly at e12.5 resulting from *Foxp4* deletion.

(F–I) Analysis of e10.5 control and (J-M) $Foxp4^{LacZ/LacZ}$ mutant spinal cords.

(N–Q) Analysis of e12.5 control and (R–U) $Foxp4^{Neo/LacZ}$ mutant cortex. N-cadherin is inversely correlated with Foxp2 and Foxp4 expression in control mice and upregulated in *Foxp4* mutants. (Q and U) $NeuN^+$ neurons form inappropriately within the VZ of the *Foxp4* mutant cortex (arrowheads in U).

(V–Y) In utero electroporation of *CMV::IRES-nEGFP* control and (Z–AC) *CMV::Foxp4-IRES-nEGFP* vectors in the e14.5 cerebral cortex suppresses N-cadherin, Sox2, and β-catenin, leading to ectopic neuronal differentiation.

(AD) Quantitation of Foxp2 and N-cadherin protein as a function of mediolateral position in control and $Foxp4^{Neo/LacZ}$ mutant cortices averaged across multiple sections.

(AE) Quantitation of the total number of spinal and cortical NPCs ($Sox2^+$) and neurons ($NeuN^+$) in *Foxp4* mutants relative to littermate controls. Mean ± SEM for multiple sections taken from 5–10 embryos for each genotype is shown. *$p < 0.05$; ***$p < 0.001$; n.s., not significant.

(AF) Quantitation of the effects of *Foxp4* misexpression on cortical neurogenesis. Plots show mean ± SEM for multiple sections taken from 5 embryos for each condition. **$p < 0.01$; ***$p < 0.001$.

See also Figure S8.

embryonic lethality (S.L. and E.E.M., unpublished data), precluding further analysis of how their combined loss affects neural development.

In e10.5 *Foxp4*$^{LacZ/LacZ}$ mutants we did not detect any overt change in N-cadherin protein staining, but the overall size of the spinal cord was reduced particularly in the MZ, as the formation of NeuN$^+$ and Tuj1$^+$ neurons was decreased by ~45% (Figures 7F–7M and 7AE). These defects were particularly evident in the differentiating Isl1/2$^+$ MNs (Figures 7I and 7M). *Foxp4*$^{LacZ/LacZ}$ mutant spinal cords also contained many neurons abnormally intermingled with Sox2$^+$ and Nestin$^+$ NPCs (Figures 7G–7I and 7K–7M), as if the cells were unable to detach from the neuroepithelium or migrate away from the VZ.

The most penetrant *Foxp4* mutant phenotypes, however, were striking disruptions in the organization of the forebrain neuroepithelium, particularly in the animals that exhibited mild to intermediate holoprosencephaly (Figures 7D, 7E, 7N–7Q, 7R–7U, S8S–S8U, and S8X–S8Z). We focused our analysis on the developing cerebral cortex as this region normally expresses both Foxp2 and Foxp4, and Foxp4 loss frequently resulted in a concomitant reduction in Foxp2 (Figures 7N, 7R, and 7AD). In this region, the Sox2$^+$ NPC compartment displayed a 2- to 3-fold increased expression of N-cadherin and the number of differentiated neurons formed was reduced by ~38% (Figures 7N–7Q, 7R–7U, and 7AE). NeuN$^+$ neurons were also interspersed within the VZ comparable to the defects seen in the *Foxp4*$^{LacZ/LacZ}$ mutant spinal cord and the chick Foxp2/4 double-knockdown experiments (Figures 2L–2O and 7H, 7L, 7Q, and 7U).

Foxp4 mutant forebrains frequently lacked lateral ventricles, with medial and lateral cortices displaying unusually contiguous contacts along their apical membranes, resulting in convolution and invagination of the neuroepithelium (Figures 7N–7P, 7R–7T, S8S–S8U, and S8X–S8Z). Sonic hedgehog, whose loss of function is commonly associated with holoprosencephaly, was nevertheless present in all embryos analyzed, and the dorsoventral position of different NPC subtypes was generally intact (Figures S8U, S8Z, and S8AA–S8AD). This feature of the *Foxp4* mutants is notably similar to the phenotype of mice in which AJ components such as Cdc42 have been inactivated (Cappello et al., 2006; Chen et al., 2006).

Finally, we misexpressed Foxp4 in the developing cortex and found that it potently suppressed the expression of N-cadherin, Sox2, β-catenin, and other components of AJs, much like the effects seen in the chick spinal cord (Figures 7V–AC and 7AF). Consequently, the number of Tbr2$^+$ neurons was elevated ~2-fold and formed ectopic clusters within and adjacent to the VZ (Figures 7Y, 7AC, and 7AF). Collectively, these results suggest that the suppressive effects of Foxp4 and Foxp2 on NPC adhesion might play a more general role in regulating progenitor maintenance throughout the developing CNS.

DISCUSSION

The polarized organization and proliferation of neuroepithelial progenitors depends on the formation of AJs between NPCs. These contacts act as a self-supporting stem cell niche to maintain cells in an undifferentiated state. Our results identify Foxp4 and Foxp2 as components of a gene regulatory network that balances the assembly and disassembly of AJs to respectively promote NPC proliferation and differentiation. In the normal course of MN development, Foxp4 levels increase as NPCs shed their adhesive contacts and migrate away from the VZ (Figure 8A). When Foxp proteins are artificially elevated, N-cadherin and Sox2 expression are suppressed, leading to the dissolution of AJs, cytoplasmic distribution of Numb, and ectopic neurogenesis within the VZ (Figure 8B). In contrast, the combined loss of Foxp2 and Foxp4 increases N-cadherin expression and retains NPCs in an undifferentiated, neuroepithelial state (Figure 8C). Together, these findings provide important insights into the developmental programs that influence how NPCs interact with themselves and their environment to regulate the size and shape of the nervous system.

Differential Expression of N-Cadherin and NPC Maintenance

N-cadherin is generally regarded as a core component of AJs that maintains the structure of the neuroepithelium throughout the CNS. Our data demonstrate that in the spinal cord, the level of N-cadherin expression is not uniform but rather varies markedly between different progenitor groups along the dorsoventral axis in accordance to their expression of Foxp4. How might discrepancies in cadherin expression affect NPC function? Studies of germline stem cells in the *Drosophila* have shown that the level of E-cadherin plays an important role in sustaining the stem cell pool and gating their differentiation behavior (Song et al., 2002; Voog et al., 2008). When E-cadherin function is blocked, germline stem cells lose contact with their niche and prematurely differentiate (Song et al., 2002; Voog et al., 2008). Remarkably, as little as 2-fold differences in E-cadherin levels can influence whether a germline stem cell remains in contact with the niche or differentiates (Jin et al., 2008). Moreover, cells that express higher levels of E-cadherin can displace other cells from the niche, thus favoring the expansion of E-cadherin^{high} cells over time (Jin et al., 2008). By analogy, groups of vertebrate NPCs that express lower or higher levels of N-cadherin might have different adhesive properties, which could similarly influence their self-renewal capacity and propensity for differentiation. The reduced expression of N-cadherin in the pMN, for example, could explain why MNs are among the first cells to differentiate in the spinal cord and why pMN cells rapidly lose their stem cell characteristics when grown in vitro compared to other progenitor groups (Mukouyama et al., 2006). The differential expression of cadherins may thus be one way in which the morphogen signals that pattern the developing nervous system ensure that different populations of NPCs expand and differentiate in a stereotyped manner.

A Transcriptional Mechanism for Regulating the Size of the Embryonic NPC Pool

In many tissues, the expansion of the stem cell pool is proportional to the size and numbers of cells that make up the niche. If the niche is enlarged or contracted, stem cell numbers are accordingly changed (Voog and Jones, 2010). In the embryonic

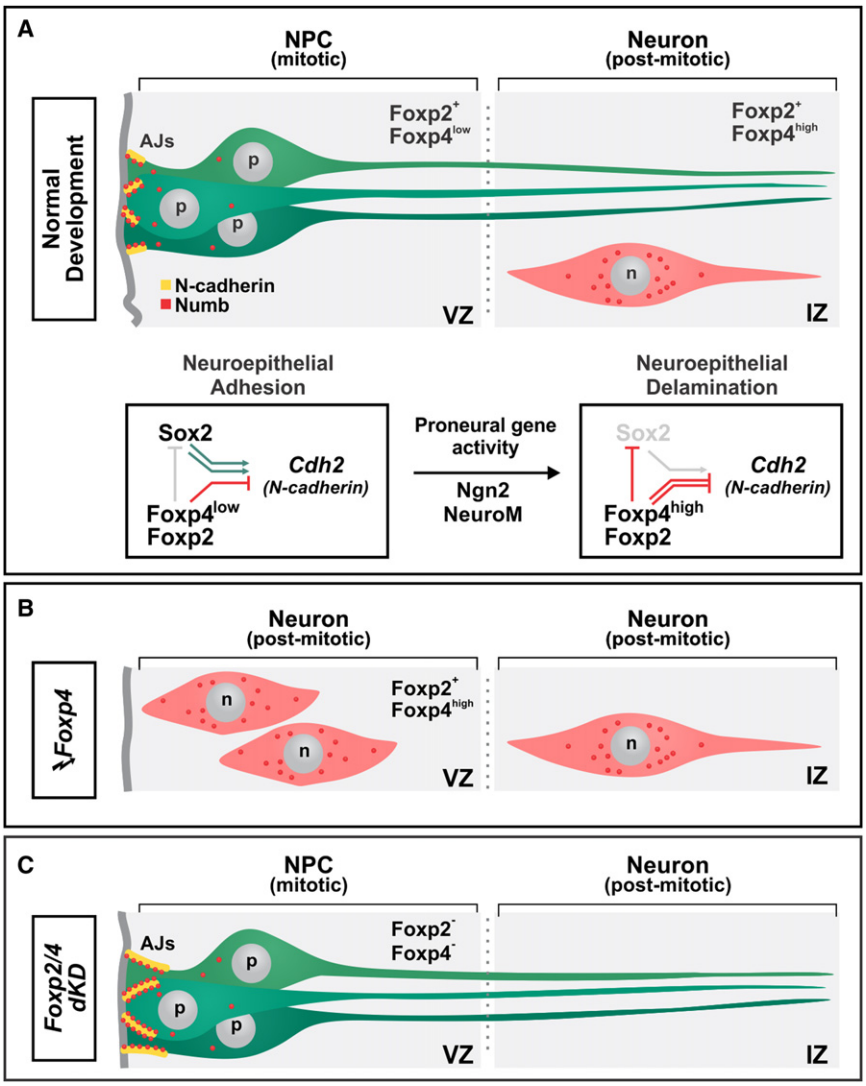

Figure 8. Opponent Activities of Foxp and Sox2 Regulate Neuroepithelial Niche Maintenance by Modulating N-Cadherin Expression

(A) Model depicting how Foxp-mediated suppression of N-cadherin offsets the progenitor maintenance activity of Sox2 and promotes neuroepithelial delamination. Sox2 provides positive inputs onto N-cadherin gene expression to maintain the neuroepithelial niche and ensure the apical localization of AJ components such as Numb.

(B) Elevated Foxp expression levels within neural progenitors eliminate N-cadherin-based AJs and promote ectopic neurogenesis.

(C) Loss of Foxp2 and Foxp4 function enhances apical AJs and maintenance of neuroepithelial progenitors.

nervous system, NPCs do not depend upon support cells; rather they form their own niche microenvironment through AJs contacts within the neuroepithelium (Zhang et al., 2010). These observations raise the question of whether there are comparable mechanisms for limiting the "size" of the NPC niche and expansion of progenitors. Our data suggest that the transcriptional regulation of N-cadherin is a means by which the embryonic NPC niche could be regulated. Previous work by Kondoh and colleagues has shown that Sox2 directly activates N-cadherin expression (Matsumata et al., 2005). Our results extend those findings by identifying Foxp4 binding sites in the *Cdh2* locus that likely mediate its repressive effects on N-cadherin. We propose that the adhesive properties of embryonic NPCs and their capacity for self-renewal depends on the balance between positive inputs on N-cadherin expression provided by Sox2 and negative inputs provided by Foxp proteins (Figure 8A). It is notable that Foxp4 can also repress Sox2, indicating that the suppression of N-cadherin may be achieved through both direct and indirect pathways.

Our results also demonstrate a similarity between the mechanism through which NPCs in the CNS detach from the neuroepithelium and the process of epithelial-mesenchymal transition carried out by neural crest progenitors. In both cases, the delamination of cells depends on both the downregulation of Sox2 activity and active repression of cadherin gene expression (Cano et al., 2000; Cimadamore et al., 2011; Taneyhill et al., 2007). Whereas neural crest cells are most dependent on the Slug/Snail family of transcriptional repressors (Cano et al., 2000; Taneyhill et al., 2007), CNS progenitors rely on Foxp proteins. The capacity to repress cadherin expression and alter cellular junctions has been seen with many other Forkhead proteins including Foxc2, Foxd3, and Foxq1 (Amorosi et al., 2008; Cheung et al., 2005; Dottori et al., 2001; Feuerborn et al., 2011; Mani et al., 2007), suggesting that this is a conserved feature of this transcription factor family.

What Are the Signals that Promote Foxp Expression?

Foxp2 is initially expressed throughout the neuroepithelium suggesting that its expression is most likely driven by broadly expressed progenitor factors. At these stages Foxp2 and Sox2 expression patterns are largely overlapping, raising the possibility that they share the same upstream activators or that Foxp2 acts downstream of Sox2 to provide a negative feedback mechanism to limit the extent of N-cadherin expression. Foxp4, by contrast, is more dynamically expressed and primarily associated with cells that are beginning to differentiate. Foxp4 elevation coincides with the onset of Ngn2 and NeuroM expression in the ventral spinal cord and is turned off as these factors are extinguished in differentiated neurons, suggesting that proneural genes act upstream of Foxp4. This hierarchical relationship is confirmed by our findings that misexpression of the Notch

effector Hes5 can suppress Foxp4 in concert with proneural gene expression. Together, these data suggest that Foxp proteins act as downstream effectors of proneural genes and mediate some of their differentiation-promoting functions. This activity is further suggested by our epistasis test, which shows that proneural gene function is compromised and cells become trapped in a neuroepithelial state when Foxp2 and Foxp4 activities are knocked down. This latter result raises the possibility that loss of Foxp function could be a contributing factor toward the formation and growth of brain cancers, as many of these tumors display neuroepithelial characteristics and Foxp proteins have previously been implicated as tumor suppressors (Banham et al., 2001; Campbell et al., 2010; Myatt and Lam, 2007).

How does the loss of Foxp2 and Foxp4 block differentiation? When Foxp2 and Foxp4 activities were reduced, N-cadherin and Sox2 protein levels were elevated and this led to a corresponding apical accumulation of proteins associated with AJs such as Numb. Numb and the related protein Numblike play an essential role in the structure of the AJ and the ability of cells to undergo asymmetric cell divisions (Cayouette and Raff, 2002; Rasin et al., 2007). In the spinal cord, Numb becomes broadly distributed throughout the cytoplasm of differentiating neurons, where it antagonizes Notch signaling and promotes neurogenesis (Wakamatsu et al., 1999). Consistent with a proneural function for Numb, we have observed that its misexpression leads to ectopic MN formation much like Foxp misexpression (D.L.R. and B.G.N., unpublished data), suggesting that the apical sequestration of Numb may be crucial for progenitor maintenance. However, it seems likely that Foxp loss acts through additional pathways. The elevation of Sox2 may be very relevant as it can antagonize proneural gene activity (Bylund et al., 2003), and it plays a central role in maintaining progenitor pluripotency in many tissues (Boiani and Schöler, 2005).

Foxp Proteins as Regulators of Cell Adhesion in Other Aspects of CNS Development

Our findings that all members of the Foxp family have the capacity to regulate cadherin expression and cell adhesion might be relevant for discerning the functions of Foxp proteins in other contexts. For example, Foxp1 is highly expressed by differentiated lateral motor column MNs. In the absence of Foxp1 function, these neurons fail to migrate laterally and do not segregate into discrete motor pools, which form the basis of spinal reflex circuits (Dasen et al., 2008; Rousso et al., 2008; Sürmeli et al., 2011). Both of these phenotypes may be partially explained by a deregulation of cadherin expression or function, as cadherin-catenin signaling has been shown to be essential for the migration of MNs along radial glial fibers, the clustering of motor pools, and further implicated in sensory-motor connectivity (Bello et al., 2012; Demireva et al., 2011). Indeed, in our experiments, we found that N-cadherin is transiently expressed in differentiated MNs, and MNs lacking Foxp2 and Foxp4 function failed to migrate laterally into the ventral horns.

Cadherins also play an important role in dendrite morphogenesis and synaptic stability in a variety of neuronal subtypes (Tanabe et al., 2006; Togashi et al., 2002). Intriguingly, Foxp4 loss disrupts the dendritic arborization of mouse Purkinje cells and their contacts with surrounding cells (Tam et al., 2011). Likewise, Foxp2 knockdown in the zebra finch brain has been reported to reduce spine density in regions associated with song acquisition (Schulz et al., 2010), and can accordingly impede vocal motor learning (Haesler et al., 2007). It is tempting to speculate that these loss-of-function phenotypes might result from abnormal cell adhesion associated with dysregulated cadherin expression or function. If true, these findings could provide a molecular explanation for the association of Foxp mutations with developmental human language and motor disorders, including autism.

EXPERIMENTAL PROCEDURES

Animal Preparation and Tissue Analysis

Olig2$^{GFP/+}$ and *Foxp4*$^{Neo/+}$ heterozygous mice were maintained as previously described (Mukouyama et al., 2006; Wang et al., 2004), following UCLA Chancellor's Animal Research Committee husbandry guidelines. *Foxp4*$^{LacZ/+}$ heterozygous mice were generated from a Bay Genomics embryonic stem cell line RRF116, which carries an insertion of a splice acceptor-β-geo reporter gene cassette between exons 5 and 6 of the *Foxp4* locus. Fertilized chicken eggs (AA Lab Eggs Inc.; McIntyre Poultry and Fertilized Eggs) were incubated at 38°C, electroporated at either e2 (HH stages 12–14) or e3 (HH stages 17–18), and collected after 6–48 hr of development as indicated in the figure legends. All embryos were fixed, cryosectioned, and processed for antibody staining or in situ hybridization histochemistry as previously described (Novitch et al., 2001; Rousso et al., 2008; Yamauchi et al., 2008). Primary antibodies and probes used are listed in the Supplemental Experimental Procedures.

Plasmid Expression and shRNA Constructs

Mouse Foxp4, mouse Foxp2, mouse Foxp1, chick Ngn2, chick Hes5-2, p27^{kip1}, chick Sox2, chick N-cadherin, chick dn-N-cad, nuclear β-gal, nuclear 6xMyc tags, and Hb9::LacZ expression vectors were either previously described or generated by subcloning the coding regions of the genes into a Gateway compatible version of the pCIG expression vector containing an IRES-nuclear-EGFP reporter (Bylund et al., 2003; Megason and McMahon, 2002; Rousso et al., 2008; Skaggs et al., 2011; Sockanathan et al., 2003). Gene knockdown was accomplished by electroporating chick embryos with a modified version of the pRFP-RNAi shRNA vector in which the RNAi cassette had been moved into pCIG (Das et al., 2006; Skaggs et al., 2011). shRNAs targeting the following sequences were used: chick *Foxp2* 3′UTR (5′-gaggata catgttctgtagaaa-3′), chick *Foxp4* CDS (5-acggagcacttaatgcaagtta-3′) or a non-targeting control (5′-cagtcgcgtttgcgactgg-3′) lacking similarity to known mammalian and chick genes (Skaggs et al., 2011).

MN and Protein Staining Quantification

The number of labeled cells per section was quantified from 12 μm cryosections sampled at 100 μm or 200 μm intervals along the rostrocaudal axis. In chick electroporation experiments, the percentage of progenitors and neurons per section was determined by dividing the number of transfected Sox2$^+$, Olig2$^+$, NeuN$^+$, or Isl1/2$^+$ cells by the total number of transfected (GFP$^+$) cells in the indicated regions of the same section or by dividing the number of cells in the transfected spinal cord by the total number on the untransfected contralateral spinal cord. In mice, percentages were determined by dividing the total number of Sox2$^+$ and NeuN$^+$ cells in *Foxp4* mutant spinal cord or cortex by the total number in littermate controls matched at the same axial position. Summarized counts were taken by averaging multiple sections from multiple embryos. In all cases, the student's t test was applied to determine the statistical significance between experimental and control groups. Foxp2, Foxp4, Sox2, and N-cadherin protein levels were measured using the ImageJ "plot profile" tool sampling > 100 pixels in diameter along the indicated tissue regions and correcting for background staining.

SUPPLEMENTAL INFORMATION

Supplemental Information includes eight figures and Supplemental Experimental Procedures and can be found with this article online at doi:10.1016/j.neuron.2012.02.024.

ACKNOWLEDGMENTS

We thank S. Butler, E. Carpenter, J. Feldman, D. Geschwind, A. Kania, S. Price, M. Sofroniew, for experimental instruction and helpful discussions; M. Cilluffo and the UCLA Brain Research Institute Electron Microscope Core; J. Briscoe, S. Butler, G. Konopka, J. Sanes, and S. Price for comments on the manuscript; M. Cayouette, J. Muhr, and S. Sockanathan for reagents. We acknowledge W. Filipiak, T. Sauders, and the Transgenic Animal Model Core of the University of Michigan's Biomedical Research Core Facilities for the preparation of the *Foxp4*^{LacZ} mice. This work was supported by the Broad Center for Regenerative Medicine and Stem Cell Research at UCLA, and grants to B.G.N. from the Whitehall Foundation (2004-05-90-APL), the Muscular Dystrophy Association (92901), and the NINDS (NS053976 and NS072804). D.L.R. was supported by the UCLA Training Program in Neural Repair (NIH T32 NS07449). C.A.P. was supported by the UCLA-California Institute for Regenerative Medicine Training Grant (TG2-01169). A.M.G. and C.P.-C. were supported by a grant from the NIMH (MH083785). S.L. and E.E.M. were supported by a grant from the NIH (HL071589).

Accepted: February 2, 2012
Published: April 25, 2012

REFERENCES

Amorosi, S., D'Armiento, M., Calcagno, G., Russo, I., Adriani, M., Christiano, A.M., Weiner, L., Brissette, J.L., and Pignata, C. (2008). FOXN1 homozygous mutation associated with anencephaly and severe neural tube defect in human athymic Nude/SCID fetus. Clin. Genet. *73*, 380–384.

Banham, A.H., Beasley, N., Campo, E., Fernandez, P.L., Fidler, C., Gatter, K., Jones, M., Mason, D.Y., Prime, J.E., Trougouboff, P., et al. (2001). The FOXP1 winged helix transcription factor is a novel candidate tumor suppressor gene on chromosome 3p. Cancer Res. *61*, 8820–8829.

Bello, S.M., Millo, H., Rajebhosale, M., and Price, S.R. (2012). Catenin-dependent cadherin function drives divisional segregation of spinal motor neurons. J. Neurosci. *32*, 490–505.

Boiani, M., and Schöler, H.R. (2005). Regulatory networks in embryo-derived pluripotent stem cells. Nat. Rev. Mol. Cell Biol. *6*, 872–884.

Briscoe, J., and Novitch, B.G. (2008). Regulatory pathways linking progenitor patterning, cell fates and neurogenesis in the ventral neural tube. Philos. Trans. R. Soc. Lond. B Biol. Sci. *363*, 57–70.

Bylund, M., Andersson, E., Novitch, B.G., and Muhr, J. (2003). Vertebrate neurogenesis is counteracted by Sox1-3 activity. Nat. Neurosci. *6*, 1162–1168.

Campbell, A.J., Lyne, L., Brown, P.J., Launchbury, R.J., Bignone, P., Chi, J., Roncador, G., Lawrie, C.H., Gatter, K.C., Kusec, R., and Banham, A.H. (2010). Aberrant expression of the neuronal transcription factor FOXP2 in neoplastic plasma cells. Br. J. Haematol. *149*, 221–230.

Cano, A., Pérez-Moreno, M.A., Rodrigo, I., Locascio, A., Blanco, M.J., del Barrio, M.G., Portillo, F., and Nieto, M.A. (2000). The transcription factor snail controls epithelial-mesenchymal transitions by repressing E-cadherin expression. Nat. Cell Biol. *2*, 76–83.

Cappello, S., Attardo, A., Wu, X., Iwasato, T., Itohara, S., Wilsch-Bräuninger, M., Eilken, H.M., Rieger, M.A., Schroeder, T.T., Huttner, W.B., et al. (2006). The Rho-GTPase cdc42 regulates neural progenitor fate at the apical surface. Nat. Neurosci. *9*, 1099–1107.

Cayouette, M., and Raff, M. (2002). Asymmetric segregation of Numb: a mechanism for neural specification from Drosophila to mammals. Nat. Neurosci. *5*, 1265–1269.

Chen, L., Liao, G., Yang, L., Campbell, K., Nakafuku, M., Kuan, C.Y., and Zheng, Y. (2006). Cdc42 deficiency causes Sonic hedgehog-independent holoprosencephaly. Proc. Natl. Acad. Sci. USA *103*, 16520–16525.

Cheung, M., Chaboissier, M.C., Mynett, A., Hirst, E., Schedl, A., and Briscoe, J. (2005). The transcriptional control of trunk neural crest induction, survival, and delamination. Dev. Cell *8*, 179–192.

Cimadamore, F., Fishwick, K., Giusto, E., Gnedeva, K., Cattarossi, G., Miller, A., Pluchino, S., Brill, L.M., Bronner-Fraser, M., and Terskikh, A.V. (2011). Human ESC-derived neural crest model reveals a key role for SOX2 in sensory neurogenesis. Cell Stem Cell *8*, 538–551.

Courchesne, E., Pierce, K., Schumann, C.M., Redcay, E., Buckwalter, J.A., Kennedy, D.P., and Morgan, J. (2007). Mapping early brain development in autism. Neuron *56*, 399–413.

Das, R.M., Van Hateren, N.J., Howell, G.R., Farrell, E.R., Bangs, F.K., Porteous, V.C., Manning, E.M., McGrew, M.J., Ohyama, K., Sacco, M.A., et al. (2006). A robust system for RNA interference in the chicken using a modified microRNA operon. Dev. Biol. *294*, 554–563.

Dasen, J.S., De Camilli, A., Wang, B., Tucker, P.W., and Jessell, T.M. (2008). Hox repertoires for motor neuron diversity and connectivity gated by a single accessory factor, FoxP1. Cell *134*, 304–316.

Demireva, E.Y., Shapiro, L.S., Jessell, T.M., and Zampieri, N. (2011). Motor neuron position and topographic order imposed by β- and γ-catenin activities. Cell *147*, 641–652.

Dorsky, R.I., Sheldahl, L.C., and Moon, R.T. (2002). A transgenic Lef1/beta-catenin-dependent reporter is expressed in spatially restricted domains throughout zebrafish development. Dev. Biol. *241*, 229–237.

Dottori, M., Gross, M.K., Labosky, P., and Goulding, M. (2001). The winged-helix transcription factor Foxd3 suppresses interneuron differentiation and promotes neural crest cell fate. Development *128*, 4127–4138.

Farkas, L.M., and Huttner, W.B. (2008). The cell biology of neural stem and progenitor cells and its significance for their proliferation versus differentiation during mammalian brain development. Curr. Opin. Cell Biol. *20*, 707–715.

Ferland, R.J., Cherry, T.J., Preware, P.O., Morrisey, E.E., and Walsh, C.A. (2003). Characterization of Foxp2 and Foxp1 mRNA and protein in the developing and mature brain. J. Comp. Neurol. *460*, 266–279.

Feuerborn, A., Srivastava, P.K., Küffer, S., Grandy, W.A., Sijmonsma, T.P., Gretz, N., Brors, B., and Gröne, H.J. (2011). The Forkhead factor FoxQ1 influences epithelial differentiation. J. Cell. Physiol. *226*, 710–719.

Feuk, L., Kalervo, A., Lipsanen-Nyman, M., Skaug, J., Nakabayashi, K., Finucane, B., Hartung, D., Innes, M., Kerem, B., Nowaczyk, M.J., et al. (2006). Absence of a paternally inherited FOXP2 gene in developmental verbal dyspraxia. Am. J. Hum. Genet. *79*, 965–972.

Ghosh, S., Marquardt, T., Thaler, J.P., Carter, N., Andrews, S.E., Pfaff, S.L., and Hunter, T. (2008). Instructive role of aPKCzeta subcellular localization in the assembly of adherens junctions in neural progenitors. Proc. Natl. Acad. Sci. USA *105*, 335–340.

Graham, V., Khudyakov, J., Ellis, P., and Pevny, L. (2003). SOX2 functions to maintain neural progenitor identity. Neuron *39*, 749–765.

Groszer, M., Keays, D.A., Deacon, R.M., de Bono, J.P., Prasad-Mulcare, S., Gaub, S., Baum, M.G., French, C.A., Nicod, J., Coventry, J.A., et al. (2008). Impaired synaptic plasticity and motor learning in mice with a point mutation implicated in human speech deficits. Curr. Biol. *18*, 354–362.

Haesler, S., Rochefort, C., Georgi, B., Licznerski, P., Osten, P., and Scharff, C. (2007). Incomplete and inaccurate vocal imitation after knockdown of FoxP2 in songbird basal ganglia nucleus Area X. PLoS Biol. *5*, e321.

Hu, H., Wang, B., Borde, M., Nardone, J., Maika, S., Allred, L., Tucker, P.W., and Rao, A. (2006). Foxp1 is an essential transcriptional regulator of B cell development. Nat. Immunol. *7*, 819–826.

Imai, F., Hirai, S., Akimoto, K., Koyama, H., Miyata, T., Ogawa, M., Noguchi, S., Sasaoka, T., Noda, T., and Ohno, S. (2006). Inactivation of aPKClambda results in the loss of adherens junctions in neuroepithelial cells without affecting neurogenesis in mouse neocortex. Development *133*, 1735–1744.

Jin, Z., Kirilly, D., Weng, C., Kawase, E., Song, X., Smith, S., Schwartz, J., and Xie, T. (2008). Differentiation-defective stem cells outcompete normal stem cells for niche occupancy in the *Drosophila* ovary. Cell Stem Cell *2*, 39–49.

Kadowaki, M., Nakamura, S., Machon, O., Krauss, S., Radice, G.L., and Takeichi, M. (2007). N-cadherin mediates cortical organization in the mouse brain. Dev. Biol. *304*, 22–33.

Lai, C.S., Fisher, S.E., Hurst, J.A., Vargha-Khadem, F., and Monaco, A.P. (2001). A forkhead-domain gene is mutated in a severe speech and language disorder. Nature *413*, 519–523.

Li, S., Weidenfeld, J., and Morrisey, E.E. (2004a). Transcriptional and DNA binding activity of the Foxp1/2/4 family is modulated by heterotypic and homotypic protein interactions. Mol. Cell. Biol. *24*, 809–822.

Li, S., Zhou, D., Lu, M.M., and Morrisey, E.E. (2004b). Advanced cardiac morphogenesis does not require heart tube fusion. Science *305*, 1619–1622.

Lu, M.M., Li, S., Yang, H., and Morrisey, E.E. (2002). Foxp4: a novel member of the Foxp subfamily of winged-helix genes co-expressed with Foxp1 and Foxp2 in pulmonary and gut tissues. Mech. Dev. *119* (*Suppl 1*), S197–S202.

Manabe, N., Hirai, S., Imai, F., Nakanishi, H., Takai, Y., and Ohno, S. (2002). Association of ASIP/mPAR-3 with adherens junctions of mouse neuroepithelial cells. Dev. Dyn. *225*, 61–69.

Mani, S.A., Yang, J., Brooks, M., Schwaninger, G., Zhou, A., Miura, N., Kutok, J.L., Hartwell, K., Richardson, A.L., and Weinberg, R.A. (2007). Mesenchyme Forkhead 1 (FOXC2) plays a key role in metastasis and is associated with aggressive basal-like breast cancers. Proc. Natl. Acad. Sci. USA *104*, 10069–10074.

Matsumata, M., Uchikawa, M., Kamachi, Y., and Kondoh, H. (2005). Multiple N-cadherin enhancers identified by systematic functional screening indicate its Group B1 SOX-dependent regulation in neural and placodal development. Dev. Biol. *286*, 601–617.

Megason, S.G., and McMahon, A.P. (2002). A mitogen gradient of dorsal midline Wnts organizes growth in the CNS. Development *129*, 2087–2098.

Meng, W., and Takeichi, M. (2009). Adherens junction: molecular architecture and regulation. Cold Spring Harb. Perspect. Biol. *1*, a002899.

Mukouyama, Y.S., Deneen, B., Lukaszewicz, A., Novitch, B.G., Wichterle, H., Jessell, T.M., and Anderson, D.J. (2006). Olig2+ neuroepithelial motoneuron progenitors are not multipotent stem cells in vivo. Proc. Natl. Acad. Sci. USA *103*, 1551–1556.

Myatt, S.S., and Lam, E.W. (2007). The emerging roles of forkhead box (Fox) proteins in cancer. Nat. Rev. Cancer *7*, 847–859.

Novitch, B.G., Chen, A.I., and Jessell, T.M. (2001). Coordinate regulation of motor neuron subtype identity and pan-neuronal properties by the bHLH repressor Olig2. Neuron *31*, 773–789.

O'Roak, B.J., Deriziotis, P., Lee, C., Vives, L., Schwartz, J.J., Girirajan, S., Karakoc, E., Mackenzie, A.P., Ng, S.B., Baker, C., et al. (2011). Exome sequencing in sporadic autism spectrum disorders identifies severe de novo mutations. Nat. Genet. *43*, 585–589.

Palmesino, E., Rousso, D.L., Kao, T.J., Klar, A., Laufer, E., Uemura, O., Okamoto, H., Novitch, B.G., and Kania, A. (2010). Foxp1 and lhx1 coordinate motor neuron migration with axon trajectory choice by gating Reelin signalling. PLoS Biol. *8*, e1000446.

Pang, T., Atefy, R., and Sheen, V. (2008). Malformations of cortical development. Neurologist *14*, 181–191.

Pariani, M.J., Spencer, A., Graham, J.M., Jr., and Rimoin, D.L. (2009). A 785kb deletion of 3p14.1p13, including the FOXP1 gene, associated with speech delay, contractures, hypertonia and blepharophimosis. Eur. J. Med. Genet. *52*, 123–127.

Rasin, M.R., Gazula, V.R., Breunig, J.J., Kwan, K.Y., Johnson, M.B., Liu-Chen, S., Li, H.S., Jan, L.Y., Jan, Y.N., Rakic, P., and Sestan, N. (2007). Numb and Numbl are required for maintenance of cadherin-based adhesion and polarity of neural progenitors. Nat. Neurosci. *10*, 819–827.

Rousso, D.L., Gaber, Z.B., Wellik, D., Morrisey, E.E., and Novitch, B.G. (2008). Coordinated actions of the forkhead protein Foxp1 and Hox proteins in the columnar organization of spinal motor neurons. Neuron *59*, 226–240.

Schulz, S.B., Haesler, S., Scharff, C., and Rochefort, C. (2010). Knockdown of FoxP2 alters spine density in Area X of the zebra finch. Genes Brain Behav. *9*, 732–740.

Shu, W., Cho, J.Y., Jiang, Y., Zhang, M., Weisz, D., Elder, G.A., Schmeidler, J., De Gasperi, R., Sosa, M.A., Rabidou, D., et al. (2005). Altered ultrasonic vocalization in mice with a disruption in the Foxp2 gene. Proc. Natl. Acad. Sci. USA *102*, 9643–9648.

Shu, W., Lu, M.M., Zhang, Y., Tucker, P.W., Zhou, D., and Morrisey, E.E. (2007). Foxp2 and Foxp1 cooperatively regulate lung and esophagus development. Development *134*, 1991–2000.

Skaggs, K., Martin, D.M., and Novitch, B.G. (2011). Regulation of spinal interneuron development by the Olig-related protein Bhlhb5 and Notch signaling. Development *138*, 3199–3211.

Sockanathan, S., Perlmann, T., and Jessell, T.M. (2003). Retinoid receptor signaling in postmitotic motor neurons regulates rostrocaudal positional identity and axonal projection pattern. Neuron *40*, 97–111.

Song, X., Zhu, C.H., Doan, C., and Xie, T. (2002). Germline stem cells anchored by adherens junctions in the Drosophila ovary niches. Science *296*, 1855–1857.

Sottocornola, R., Royer, C., Vives, V., Tordella, L., Zhong, S., Wang, Y., Ratnayaka, I., Shipman, M., Cheung, A., Gaston-Massuet, C., et al. (2010). ASPP2 binds Par-3 and controls the polarity and proliferation of neural progenitors during CNS development. Dev. Cell *19*, 126–137.

Stepniak, E., Radice, G.L., and Vasioukhin, V. (2009). Adhesive and signaling functions of cadherins and catenins in vertebrate development. Cold Spring Harb. Perspect. Biol. *1*, a002949.

Sürmeli, G., Akay, T., Ippolito, G.C., Tucker, P.W., and Jessell, T.M. (2011). Patterns of spinal sensory-motor connectivity prescribed by a dorsoventral positional template. Cell *147*, 653–665.

Takahashi, K., Liu, F.C., Hirokawa, K., and Takahashi, H. (2003). Expression of Foxp2, a gene involved in speech and language, in the developing and adult striatum. J. Neurosci. Res. *73*, 61–72.

Takahashi, K., Liu, F.C., Hirokawa, K., and Takahashi, H. (2008). Expression of Foxp4 in the developing and adult rat forebrain. J. Neurosci. Res. *86*, 3106–3116.

Tam, W.Y., Leung, C.K., Tong, K.K., and Kwan, K.M. (2011). Foxp4 is essential in maintenance of Purkinje cell dendritic arborization in the mouse cerebellum. Neuroscience *172*, 562–571.

Tamura, S., Morikawa, Y., Iwanishi, H., Hisaoka, T., and Senba, E. (2003). Expression pattern of the winged-helix/forkhead transcription factor Foxp1 in the developing central nervous system. Gene Expr. Patterns *3*, 193–197.

Tamura, S., Morikawa, Y., Iwanishi, H., Hisaoka, T., and Senba, E. (2004). Foxp1 gene expression in projection neurons of the mouse striatum. Neuroscience *124*, 261–267.

Tanabe, K., Takahashi, Y., Sato, Y., Kawakami, K., Takeichi, M., and Nakagawa, S. (2006). Cadherin is required for dendritic morphogenesis and synaptic terminal organization of retinal horizontal cells. Development *133*, 4085–4096.

Taneyhill, L.A., Coles, E.G., and Bronner-Fraser, M. (2007). Snail2 directly represses cadherin6B during epithelial-to-mesenchymal transitions of the neural crest. Development *134*, 1481–1490.

Togashi, H., Abe, K., Mizoguchi, A., Takaoka, K., Chisaka, O., and Takeichi, M. (2002). Cadherin regulates dendritic spine morphogenesis. Neuron *35*, 77–89.

Voog, J., and Jones, D.L. (2010). Stem cells and the niche: a dynamic duo. Cell Stem Cell *6*, 103–115.

Voog, J., D'Alterio, C., and Jones, D.L. (2008). Multipotent somatic stem cells contribute to the stem cell niche in the Drosophila testis. Nature *454*, 1132–1136.

Wakamatsu, Y., Maynard, T.M., Jones, S.U., and Weston, J.A. (1999). NUMB localizes in the basal cortex of mitotic avian neuroepithelial cells and modulates neuronal differentiation by binding to NOTCH-1. Neuron *23*, 71–81.

Wang, B., Weidenfeld, J., Lu, M.M., Maika, S., Kuziel, W.A., Morrisey, E.E., and Tucker, P.W. (2004). Foxp1 regulates cardiac outflow tract, endocardial cushion morphogenesis and myocyte proliferation and maturation. Development *131*, 4477–4487.

Yamauchi, K., Phan, K.D., and Butler, S.J. (2008). BMP type I receptor complexes have distinct activities mediating cell fate and axon guidance decisions. Development *135*, 1119–1128.

Zechner, D., Fujita, Y., Hülsken, J., Müller, T., Walther, I., Taketo, M.M., Crenshaw, E.B., 3rd, Birchmeier, W., and Birchmeier, C. (2003). beta-Catenin signals regulate cell growth and the balance between progenitor cell expansion and differentiation in the nervous system. Dev. Biol. *258*, 406–418.

Zhang, J., Woodhead, G.J., Swaminathan, S.K., Noles, S.R., McQuinn, E.R., Pisarek, A.J., Stocker, A.M., Mutch, C.A., Funatsu, N., and Chenn, A. (2010). Cortical neural precursors inhibit their own differentiation via N-cadherin maintenance of beta-catenin signaling. Dev. Cell *18*, 472–479.